Quantum Electronics **48** (4) 325–331 (2018)

https://doi.org/10.1070/QEL16637

Suppression of small-scale self-focusing of high-power laser beams due to their self-filtration during propagation in free space

V.N. Ginzburg, A.A. Kochetkov, A.K. Potemkin, E.A. Khazanov

Abstract. **It has been experimentally confirmed that self-cleaning of a laser beam from spatial noise during propagation in free space makes it possible to suppress efficiently the self-focusing instability without applying spatial filters. Measurements of the instability increment by two independent methods have demonstrated quantitative agreement with theory and high efficiency of small-scale self-focusing suppression. This opens new possibilities for using optical elements operating in transmission (frequency doublers, phase plates, beam splitters, polarisers, etc.) in beams with intensities on the order of a few TW cm^{-2}.**

Keywords: *small-scale self-focusing, high-power femtosecond laser beams, self-filtration.*

1. Introduction

Lasers with tera- and petawatt peak powers have become very popular in recent years due to their wide application range. Generally, a laser beam emerging from a compressor is directed onto a target by means of one or several mirrors; transmission optical elements operating are not used in this case. The reason is as follows: at an unfocused beam intensity on the order of ~1 TW cm^{-2}, which is typical of high-power femtosecond lasers, small-scale self-focusing (SSSF) arises in optical elements with a thickness of 1 mm or more [1], which leads to irreversible destruction of these elements. At the same time, to control laser beam parameters, one needs specifically optical elements operating in transmission: frequency doublers, phase plates, beam splitters, polarisers, and nonlinear optical elements extending the pulse spectrum. It is the SSSF effect that limits the application of all these elements.

The key parameter determining the SSSF is the nonlinear phase shift, referred to as the B integral:

$$B = k\gamma Il, \tag{1}$$

where I is the radiation intensity; k is the wave number; l is the length of the medium; and γ is the nonlinearity coefficient of the medium, which is determined by the diagonal component of the nonlinear susceptibility tensor $\chi^{(3)}$. At large values of the B integral ($B > 3$), SSSF leads to strong modulation of the beam intensity and destruction of optical elements, as was confirmed in many experiments.

In physical essence, SSSF is amplification of small-scale spatial perturbations (noise amplification) in the field of an intense plane wave. The B-integral value determines the gain. The maximum gain and instability range (range of spatial frequencies for which this gain exceeds unity) were found in Bespalov and Talanov's pioneer study [1]. An exact calculation of the gain as a function of spatial frequency (or angle α between the wave vectors of noise and plane wave) and the phase of the noise component at the input of a nonlinear medium was performed in [2] for a linearly polarised beam and in [3, 4] for arbitrarily polarised beams. Thus, the noise level at the output of optical element is determined by the noise level at its input and the B-integral value.

To suppress SSSF, one must primarily reduce the B-integral value; however, when the intensity I is high, it is necessary to use very thin optical elements [see (1)], which are rather difficult to fabricate. For the same reason, division of a nonlinear element into two, a widespread procedure for nanosecond lasers [5–7], is not used in high-power femtosecond lasers. Circular polarisation, for which the effective value of the B integral in both isotropic media [2, 3, 8, 9] and ceramics [10] is smaller by a factor of 1.5 than for linear polarisation, is very rarely applied in high-power lasers. It was shown in [11, 12] that the effective value of the B integral can also be reduced by choosing properly the cubic crystal orientation.

Another way to suppress SSSF is to reduce the small-scale spatial noise of the laser beam at the input of the medium. A conventional way to clean the beam from noise is to use spatial filters [13–15]. The point is that the noises propagating at the angle [1]

$$\alpha_{\max} = \sqrt{2n\gamma I}\,, \tag{2}$$

where n is the refractive index of the medium, are most strongly amplified. Hereinafter, we consider angles α outside the nonlinear medium rather than inside. A diaphragm mounted in the focal waist of the telescope makes it possible to cut off perturbations propagating at angles $\alpha \approx \alpha_{\max}$ and transmit the main diffraction beam without attenuation. However, it appears rather difficult to apply spatial filters in order to suppress SSSF for beams with intensities on the order of few TW cm^{-2}, because SSSF makes it impossible to use lens telescopes.

An original beam cleanup technique was proposed in [16] to suppress SSSF for petawatt radiation: self-filtration of a beam propagating through free space. If an optical element is located at a large distance from a noise source, the most 'hazardous' noise components (at $\alpha \approx \alpha_{\max}$) leave the beam aper-

V.N. Ginzburg, A.A. Kochetkov, A.K. Potemkin, E.A. Khazanov
Institute of Applied Physics, Russian Academy of Sciences,
ul. Ul'yanova 46, 603950 Nizhny Novgorod, Russia;
e-mail: vlgin@rambler.ru

Received 16 February 2018
Kvantovaya Elektronika **48** (4) 325–331 (2018)
Translated by Yu.P. Sin'kov

ture (Fig. 1). In this case, the free space works as a spatial filter. The main sources of harmonic perturbations are the surfaces of mirrors or diffraction gratings; therefore, having placed an optical element at a sufficiently large distance L from the last mirror, one can remove the 'hazardous' noise components from the region of interaction with a strong wave. To this end, the following condition must be satisfied:

$$L > L_{sc} = D/\alpha_{max}, \quad (3)$$

where D is the beam diameter and L_{sc} is the characteristic length, beginning with which self-cleaning becomes efficient. The spatial noise present in the beam before the reflection from mirror (*1*) is also filtered off, because the distance to nonlinear element (*2*) for this noise component is even larger, and condition (3) is obviously satisfied. It follows from expression (2) that the angle α_{max} is proportional to the root square of beam intensity and is independent of the B integral. The characteristic beam intensity for nanosecond lasers is few GW cm^{-2}, which yields $\alpha_{max} \approx 1$ mrad and makes self-filtration in free space impossible because of a too large L value. In the case of femtosecond lasers, the intensity amounts to a few TW cm^{-2}, and the angle α_{max} is significantly larger (several tens of mrad), which leads to reasonable values of distance L even for large diameters D.

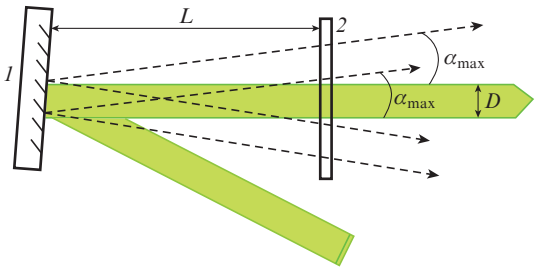

Figure 1. Self-filtration of a beam propagating in free space: (*1*) mirror or diffraction grating and (*2*) nonlinear element.

The effect of self-filtration of intense radiation was confirmed in a qualitative experiment [16, 17], where the degree of destruction of glass by SSSF at different L values was investigated. The purpose of this study was to confirm quantitatively the suppression of self-focusing of intense laser radiation by measuring the spatial spectrum of the noise gain as a function of distance L to the noise source.

2. Schematic of the experiment

The spatial noise gain was measured by two independent methods: direct [5, 18] (Fig. 2a) and indirect [18] (Fig. 2b). In both cases the radiation source was the front-end of the PEARL laser [19]. To form a beam with a quasi-homogeneous transverse profile but without sharp boundaries, diaphragm (*1*) (2 mm in diameter) was installed at the input of spatial filter with double magnification, located before the compressor. The radiation energy at the compressor output was 0.5 mJ, and the characteristic pulse duration was 70 fs. The α_{max} value was calculated from formula (2) to be 7.8 mrad, and the B value was 1.4. Thin (0.2 mm), slightly matte glass plate (*2*) was used as a spatial noise source. The lateral intensity distributions in the near-field zone before and after passing through the plate are presented in Figs 2c and 2d. Nonlinear element (*3*) was a 10-mm-thick glass plate, after which the beam intensity decreased by a factor of 25 due to the reflection from the front face of glass wedge (4). This reduction was used to exclude the air breakdown in the focal plane (see below).

To measure directly the gain (Fig. 2a), the laser beam was focused by spherical mirror (*5*) with a focal length of 280 mm. As in [5, 12, 18], plane mirror (*6*) with a hole 2 mm in diameter was located in the focal plane to cut off the main (noise-free) beam. The hole diameter was sufficiently large to let the main beam pass completely (including wings) through the hole and provide reflection of only the noise component (shown by dashed lines) from mirror (*6*). Lens (*7*) transferred an image from mirror (*6*) to CCD camera (*8*). Thus, the CCD camera recorded the angular noise spectrum with a 'cut-off' range of angles smaller than 1/280 = 3.6 mrad. The noise gain $G(\alpha)$ was calculated using normalisation. The distance L between nonlinear element (*3*) and noise source (*2*) was varied in the range of 20–600 mm.

A schematic of the experiment with indirect measurement of gain is shown in Fig. 2b. The beam transmitted through the nonlinear element arrived at lens (*9*) with a focal length of 580 mm, which transferred the image from the output plane of noise source (*2*) to CCD camera (*10*). It was shown in [18] that the noise gain spectrum $G(\alpha)$ beyond the region of paraxial rays can be calculated from the formula

$$G(\alpha)\cos^2\psi_n(\alpha) = |S(\alpha)|^2/|S_0(\alpha)|^2, \quad (4)$$

where ψ_n is the nonlinear phase (the expressions for this parameter can be found in [5, 18]) and $S(\alpha)$ [$S_0(\alpha)$] is the spatial intensity spectrum of the noise source image transferred through the nonlinear [linear] element, i.e., the spatial intensity spectrum of the beam recorded by CCD camera (*10*). Thus, having found the Fourier spectrum of the intensity distribution on camera (*10*), one can calculate $G(\alpha)$. The positions of noise source (*2*), lens (*9*), and CCD camera (*10*) were fixed, and the distance L was varied in the range of 12–570 mm.

3. Results and discussion

3.1. Direct measurement of spatial noise gain

First, the angular noise spectrum was measured in the linear regime ($B = 0$), i.e., without amplification (Fig. 3a). To this end, the laser pulse duration was multiply increased by changing significantly the compressor base, which gave rise to a negligible nonlinearity in the glass plate. Then we changed the distance L between the noise source and nonlinear element in the nonlinear mode ($B = 1.4$) (Figs 3b–3h). Using the measurement results, we calculated the noise gain spectrum for each L value and then the averaged (over azimuthal angle) G value as a function of angle α. The thus obtained dependences $G(\alpha)$ are presented in Fig. 3 in the right column, which also contains theoretical dependences $G(\alpha)$ (calculated according to the SSSF theory [2], with self-filtration disregarded).

According to the SSSF theory, the noise gain depends not only on the angle α between the wave vectors of the strong and noise waves but also on the phase difference ψ between these waves at the input of the nonlinear medium.

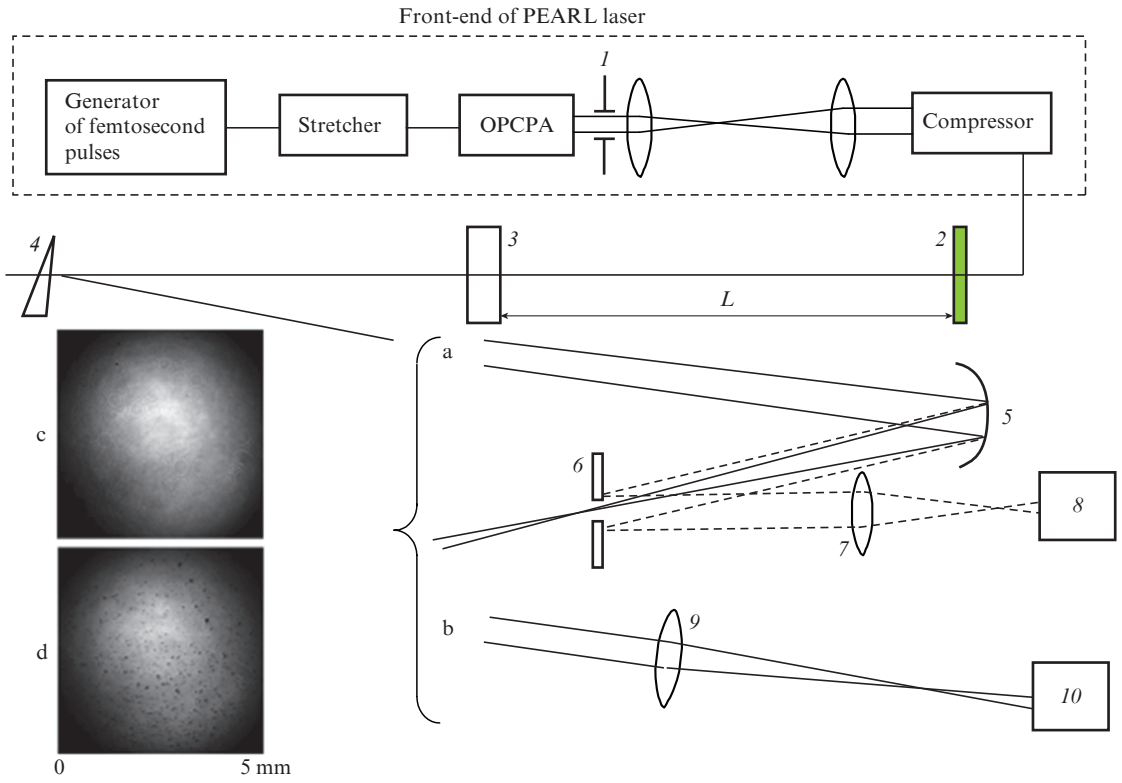

Figure 2. Schematic of the experiment for (a) direct and (b) indirect measurements of spatial noise gain and beam intensity distributions (c) before and (d) after the beam transmission through noise source *2*: (*1*) diaphragm; (*2*) noise source (thin matte plate); (*3*) nonlinear element; (*4*) glass wedge; (*5*) spherical mirror; (*6*) mirror with a hole; (*7*, *9*) lenses; (*8*, *10*) CCD cameras.

The phase difference ψ, in turn, depends on the angle α in correspondence with the evident formula $\psi = \pi\alpha^2 L/\lambda$, where λ is wavelength. Here, we consider the matte plate as an ideal amplitude mask; therefore, this phase difference in the noise source plane is zero for all α values. Thus, the dependence of G on ψ leads to modulation of the function $G(\alpha)$, i.e., the occurrence of rings in the far-field zone of amplified noise (Figs 3b, 3c). The frequency of oscillations of $G(\alpha)$ increases with an increase in L [2, 5], and finally the rings in the far-field noise zone become indistinguishable (Figs 3d–3h).

Figures 3b–3e demonstrate good agreement between the measured and theoretical dependences $G(\alpha)$; the smaller (as compared with theoretically predicted) modulation depth of the experimental curves in Figs 3b and 3c is due to the insufficiently high angular resolution of the optics used in the experiment. This coincidence of dependences is observed at relatively small values $L < L_{sc} =$ 320 mm, which are insufficient for self-filtration. Here, we assumed the beam diameter to be $D = 2.5$ mm. At $L =$ 400 mm or more (Figs 3f–3h), condition (3) is satisfied, and the measured noise gain G is much smaller than the theoretical value, found for an optical element unlimited in the transverse direction (i.e., with self-filtration disregarded). For clarity, the angles α_{sc} at which $L = L_{sc}$ are indicated by dashed lines in Figs 3d–3h.

Thus, as was predicted, the range of the angular spectrum in which amplification occurs narrows with an increase in L, and the noise amplification almost completely stops at $L = 600$ mm. In other words, we experimentally demonstrated self-filtration of laser radiation and SSSF suppression.

3.2. Indirect measurement of spatial noise gain

In the case of indirect measurement of noise gain [18], we transferred the image from the plane of noise source (*2*) to CCD camera (*10*) through nonlinear element (*3*) (see Fig. 2b). The images obtained and their spatial Fourier spectra are shown in Fig. 4a on the left and in the middle, respectively. The experimental [plotted using formula (4)] and theoretical (calculated from the formulas reported in [5, 18]) dependences of the function $G\cos^2\psi_n$ on the angle α are presented in Fig. 4 (on the right).

First, we will analyse the distributions recorded by CCD camera (*10*) (Fig. 4, on the left). In the case of conventional, linear ($B = 0$) image transfer, one can see dark dots with sharp boundaries (Fig. 4a). If the image is transferred through the nonlinear element located at a small distance L (Figs 4b–4d), i.e., at a viewing angle exceeding $\alpha_{max} = 7.8$ mrad, small bright dots arise in the image. The pattern significantly changes with an increase in distance L: bright dots disappear (Figs 4e, 4f), and, at even larger L values, the beam becomes smooth in the higher intensity region (Fig. 4g). Thus, even a qualitative analysis in the near-field zone confirms the occurrence of self-focusing suppression.

Note that, at a large distance L (i.e., when $L > L_{sc}$) many noise rays pass beyond the nonlinear element aperture; this circumstance, at first glance, should lead to an ideal (i.e., as in the linear case) image transfer. However, as follows from a comparison of the near-field zones in Figs 4a and 4g, this is not true. There are no dark dots with sharp boundaries in the main part of the beam in Fig. 4g. The reason is that the noise rays in the CCD camera plane interfere with the main wave, propagating at an angle $\alpha = 0$ and accumulating, in contrast to the linear case (Fig. 4a), a nonlinear phase equal to the B

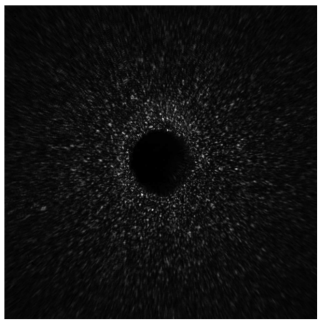

–16 mrad 16 mrad

L – arbitrary

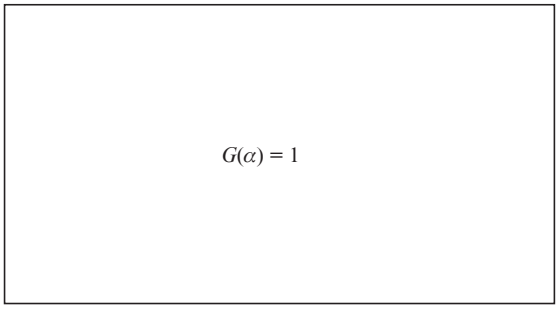

a

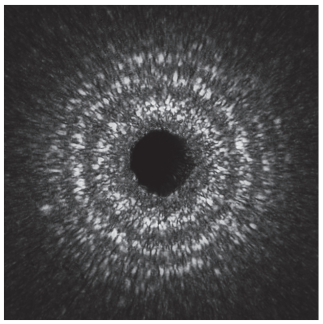

–16 mrad 16 mrad

L = 20 mm

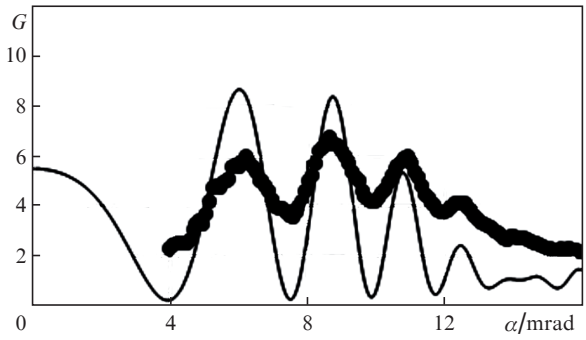

b

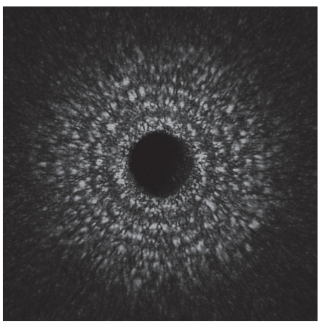

–16 mrad 16 mrad

L = 40 mm

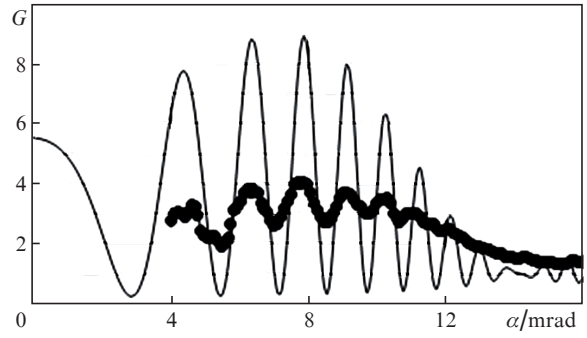

c

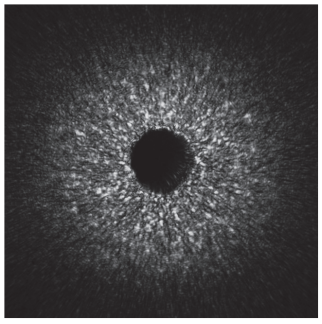

–16 mrad 16 mrad

L = 200 mm

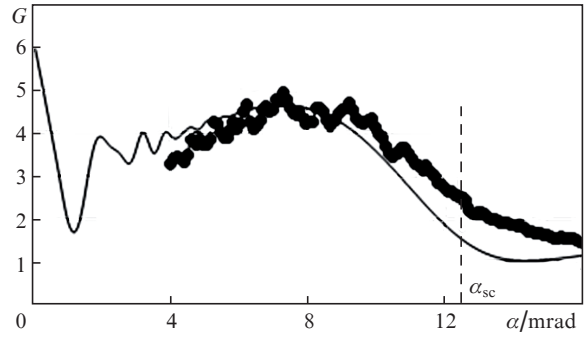

d

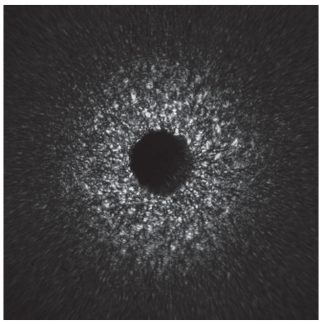

–16 mrad 16 mrad

L = 250 mm

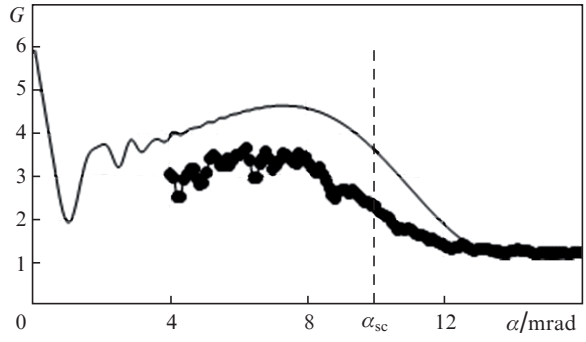

e

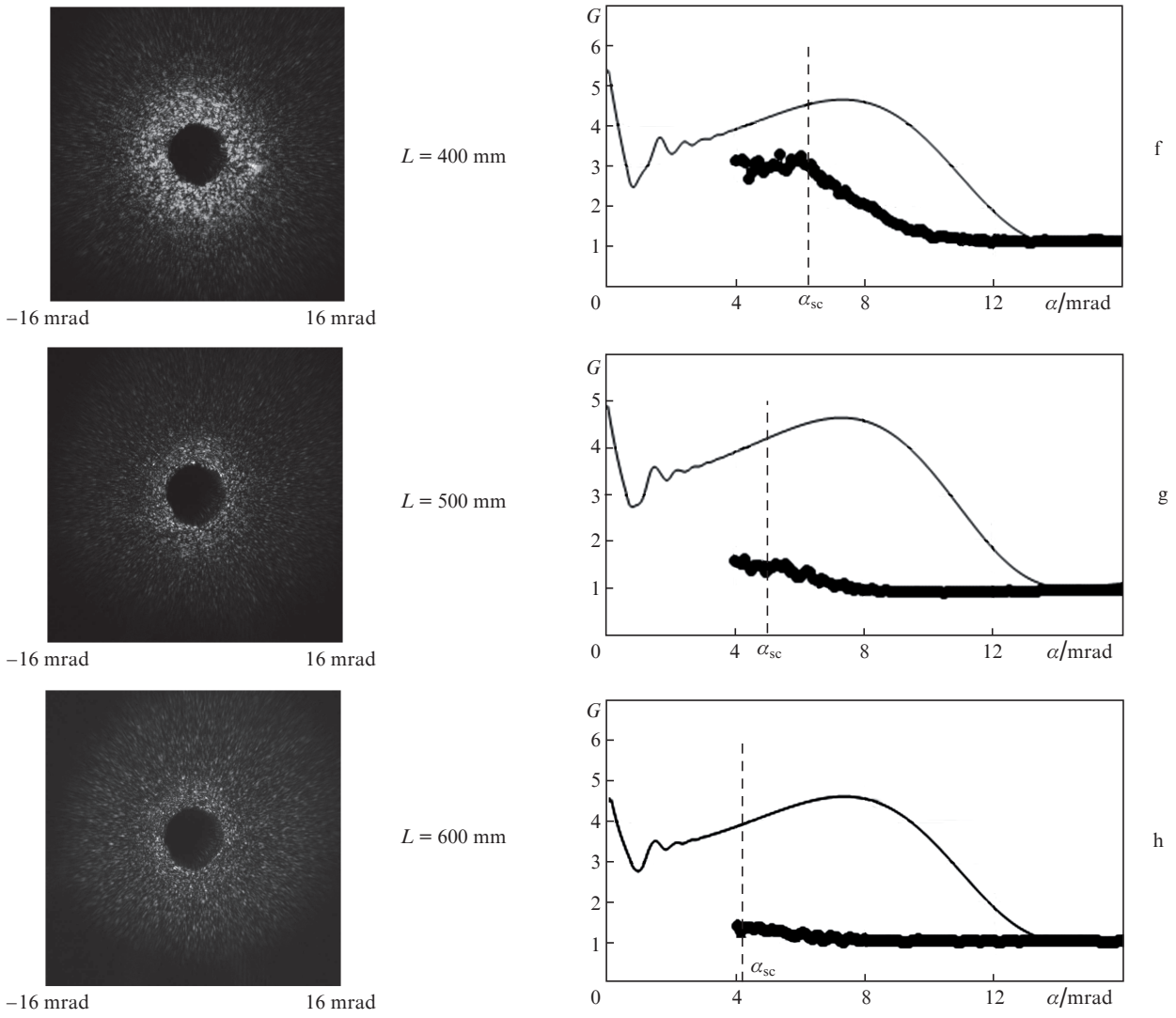

Figure 3. Angular noise spectra (on the left) and experimental (dots) and calculated (thin curves) dependences of noise gain on angle α (on the right) at B = (a) 0 and (b–h) 1.4 for different L values.

integral. The main-wave intensity is much lower at the beam periphery; i.e., the nonlinear phase is small and, therefore, the image transfer is close to ideal. Specifically for this reason clearly limited dark dots are observed at the beam periphery in Fig. 4g.

Second, we will consider the noise (high-frequency) intensity spectra and the gain spectra presented in Fig. 4 (in the middle and on the right, respectively). In the case of conventional, linear ($B = 0$) image transfer, the noise spectrum is a monotonic function of two coordinates (Fig. 4a). At B = 1.4 and small lengths L (Figs 4b–4d), characteristic bright or dark rings arise in the spectrum, which correspond to the angles at which the noise gain is maximum or minimum. The dependences in Fig. 4b demonstrate good coincidence between the experimental and theoretical data; the smaller (than the theoretically predicted) modulation depth is due to the insufficiently high angular resolution of the optics used in the experiment. A further increase in distance L (Figs 4d–4g) reduces the distance between the rings so that they merge. The theoretical curves in Figs 4d–4g are smoothed for clarity. Consistency with theoretical data is observed at relatively small L values. At L = 100 mm, agreement is retained for only small angles α, whereas at large α values the measured noise gain G is smaller than its theoretical value, found for a laterally unbounded optical element (i.e., with self-filtration disregarded). At L = 200 mm or more (Figs 4e–4g), the discrepancy between the experiment and theory becomes significant for practically all α values: one can observe a great decrease in gain and suppression of self-focusing. For clarity, the angles α_{sc} at which $L = L_{sc}$ are indicated by dashed lines in Figs 4e–4g.

Numerical simulation of the propagation of a noisy beam in a nonlinear medium using the Fresnel program [14] confirmed that self-focusing is suppressed. Thus, both indirect and direct measurements of noise gain showed that the angular spectrum region in which amplification occurs narrows with an increase in L; the amplification is significantly suppressed at $L = L_{sc}$, and self-focusing almost completely disappears with a further increase in L. Note that in the case of indirect measurements of $G(\alpha)$ (i.e., when the $|S(\alpha)|^2/|S_0(\alpha)|^2$ value is measured, self-filtration of radiation and self-focusing suppression are observed even at L values smaller than in direct measurements of $G(\alpha)$ (compare the right parts of Figs 3 and 4).

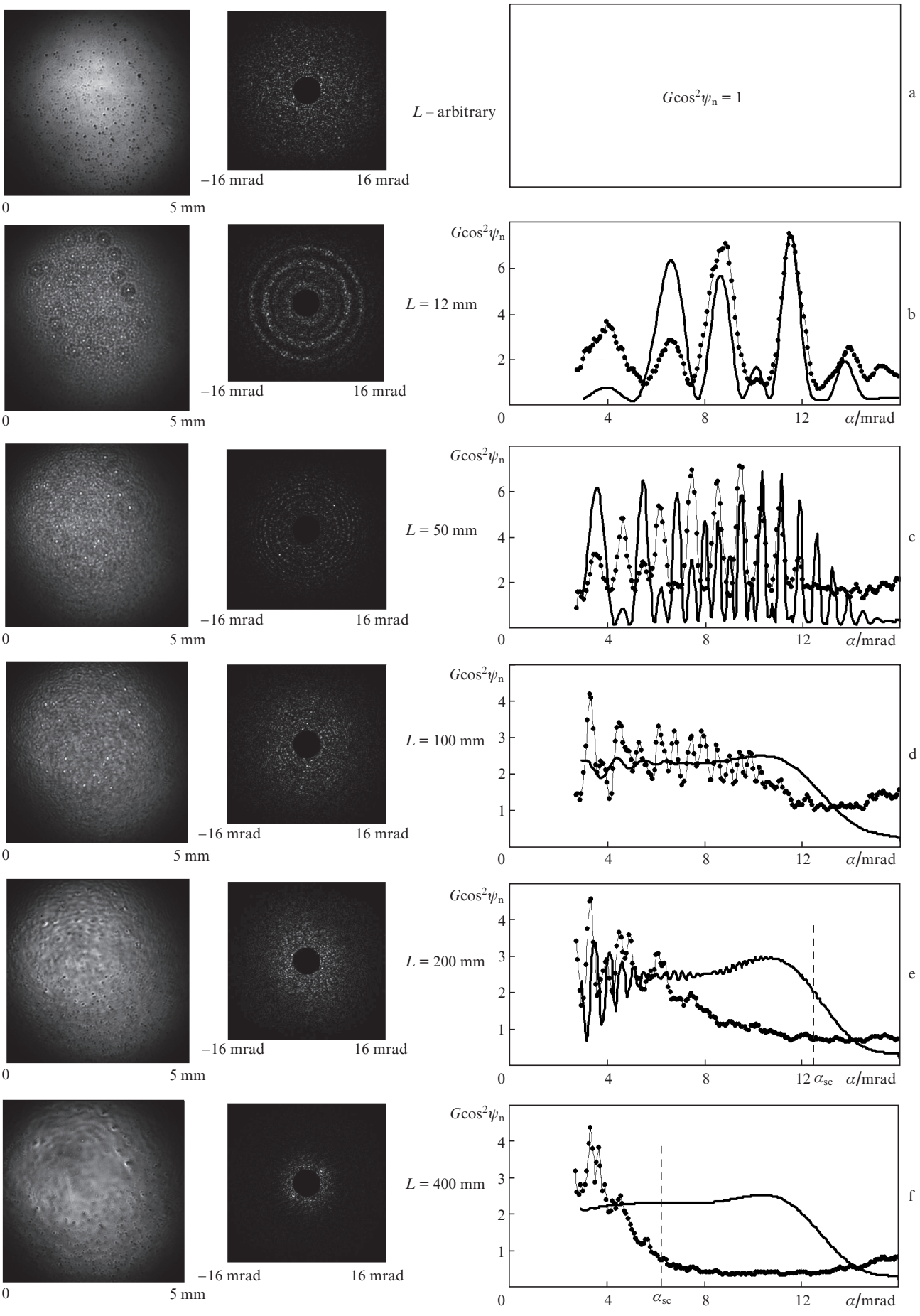
L – arbitrary
Gcos²ψn = 1
a
–16 mrad
16 mrad
0
5 mm
L = 12 mm
Gcos²ψn
b
L = 50 mm
c
L = 100 mm
d
L = 200 mm
e
L = 400 mm
f
α/mrad
αsc

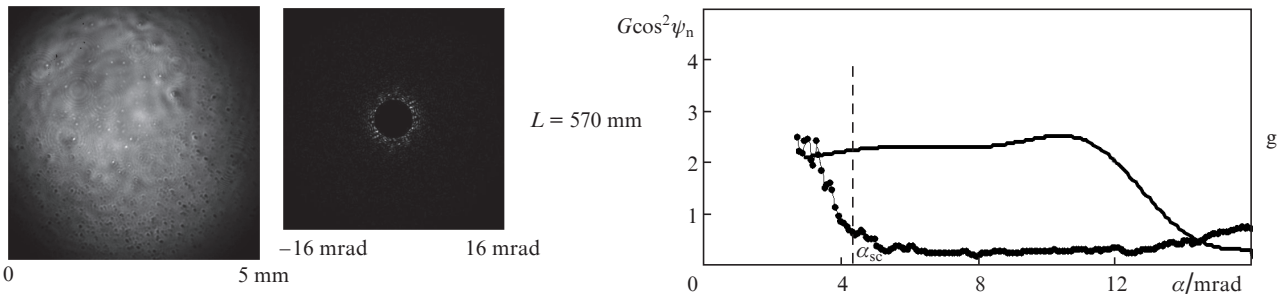

Figure 4. Intensity distributions recorded by CCD camera (*10*) (on the left), spatial spectra (in the middle), and experimental (dots) and theoretical (lines) dependences of noise gain on angle α (on the right) at B = (a) 0 and (b–g) 1.4 for different L values.

4. Conclusions

Thus, we experimentally confirmed the possibility of suppressing SSSF using the self-filtration of a femtosecond laser beam propagating in free space. The spatial noise gain (increment of self-focusing instability) was measured by two independent methods. In both cases we obtained quantitative agreement between experimental and theoretical data and demonstrated high efficiency of self-focusing suppression. It was shown that transmission optical elements can be used for beams with intensity on the order of a few TW cm^{-2}. This circumstance significantly expands the possibilities of controlling parameters of tera- and petawatt laser pulses, for example in second-harmonic conversion, transformation of linear polarisation into circular, controlled broadening of pulse spectrum with its subsequent recompression, beam splitting into two, etc.

Acknowledgements. This work was performed within the Programme of Development of the Institute of Applied Physics, Russian Academy of Sciences, for 2016–2020 (Agreement No. 007-021225/2) and by the Presidium of RAS (Programme 'Extreme Light Fields and Their Interaction with Matter').

References

1. Bespalov V.I., Talanov V.I. *Pis'ma Zh. Eksp. Teor. Fiz*., **3**, 471 (1966).
2. Rozanov N.N., Smirnov V.A. Sov. *J. Quantum Electron*., **10**, 232 (1980) [*Kvantovaya Elektron*., **7**, 410 (1980)].
3. Vlasov S.N., Talanov V.I. *Samofokusirovka voln* (Wave Self-Focusing) (Nizhny Novgorod: Izd-vo IPF RAN, 1997).
4. Kuz'mina M.S., Khazanov E.A. *Quantum Electron*., **43**, 936 (2013) [*Kvantovaya Elektron*., **43**, 936 (2013)].
5. Poteomkin A.K., Martyanov M.A., Kochetkova M.S., Khazanov E.A. *IEEE J. Quantum Electron*., **45**, 336 (2009).
6. Vlasov S.N. *Sov. J. Quantum Electron*, **6**, 245 (1976) [*Kvantovaya Elektron*., **3**, 451 (1976)].
7. Vlasov S.N., Yashin V.E. *Sov. J. Quantum Electron*., **11**, 313 (1981) [*Kvantovaya Elektron*., **8**, 510 (1981)].
8. Poteomkin A.K., Khazanov E.A., Martyanov M.A., Kirsanov A.V., Shaykin A.A. *IEEE J. Quantum Electron*., **45**, 854 (2009).
9. Kuz'mina M.S., Khazanov E.A. *Quantum Electron*., **43**, 21 (2013) [*Kvantovaya Elektron*., **43**, 21 (2013)].
10. Khazanov E.A., Maslennikov O.V., Ginzburg V.N., Kochetkov A.A., Nekorkin V.I. *Opt. Express*, **25**, 27968 (2017).
11. Kuz'mina M.S., Khazanov E.A. *Izv. Vyssh. Uchebn. Zaved., Ser. Radiofiz*., **59**, 596 (2016).
12. Ginzburg V.N., Kochetkov A.A., Kuz'mina M.S., Burdonov K.F., Shaikin A.A., Khazanov E.A. *Quantum Electron*., **47**, 248 (2017) [*Kvantovaya Elektron*., **47**, 248 (2017)].
13. Kuz'mina M.S., Rozanov N.N., Smirnov V.A. *Opt. Spektrosk*., **51**, 509 (1981).
14. Garanin S.G., Epatko I.V., L'vov L.V., Serov R.V., Sukharev S.A. *Quantum Electron*., **37**, 1159 (2007) [*Kvantovaya Elektron*., **37**, 1159 (2007)].
15. Poteomkin A.K., Barmashova T.V., Kirsanov A.V., Martyanov M.A., Khazanov E.A., Shaykin A.A. *Appl. Opt*., **46**, 4423 (2007).
16. Mironov S.Y., Lozhkarev V.V., Ginzburg V.N., Yakovlev I.V., Luchinin G., Shaykin A.A., Khazanov E.A., Babin A.A., Novikov E., Fadeev S., Sergeev A.M., Mourou G.A. *IEEE J. Sel. Top. Quantum Electron*., **18**, 7 (2012).
17. Mironov S., Lozhkarev V., Luchinin G., Shaykin A., Khazanov E. *Appl. Phys. B: Lasers and Optics*, **113**, 147 (2013).
18. Kochetkova M.S., Mart'yanov M.A., Potemkin A.K., Khazanov E.A. *Quantum Electron*., **39**, 923 (2009) [*Kvantovaya Elektron*., **39**, 923 (2009)].
19. Lozhkarev V.V., Freidman G.I., Ginzburg V.N., Katin E.V., Khazanov E.A., Kirsanov A.V., Luchinin G.A., Mal'shakov A.N., Martyanov M.A., Palashov O.V., Poteomkin A.K., Sergeev A.M., Shaykin A.A., Yakovlev I.V., Garanin S.G., Sukharev S.A., Rukavishnikov N.N., Charukhchev A.V., Gerke R.R., Yashin V.E. *Opt. Express*, **14**, 446 (2006).